Journal of Colloid and Interface Science 567 (2020) 18–27

Contents lists available at ScienceDirect

Journal of Colloid and Interface Science

journal homepage: www.elsevier.com/locate/jcis

Dynamic interfacial tension measurement under electric fields allows detection of charge carriers in nonpolar liquids

Rajarshi Sengupta, Aditya S. Khair, Lynn M. Walker *

Department of Chemical Engineering, Carnegie Mellon University, Pittsburgh, PA 15213, USA

HIGHLIGHTS

- Surfactant transport to oil-water interfaces is enhanced under electric fields.
- Electrophoresis of surfactant-induced aggregates enhances transport.
- Measuring transport under electric fields detects charge carriers in oil phases.
- Surfactant transport in the aqueous phase is not influenced by electric fields.
- Electric fields do not affect the equilibrium interfacial tension.

GRAPHICAL ABSTRACT

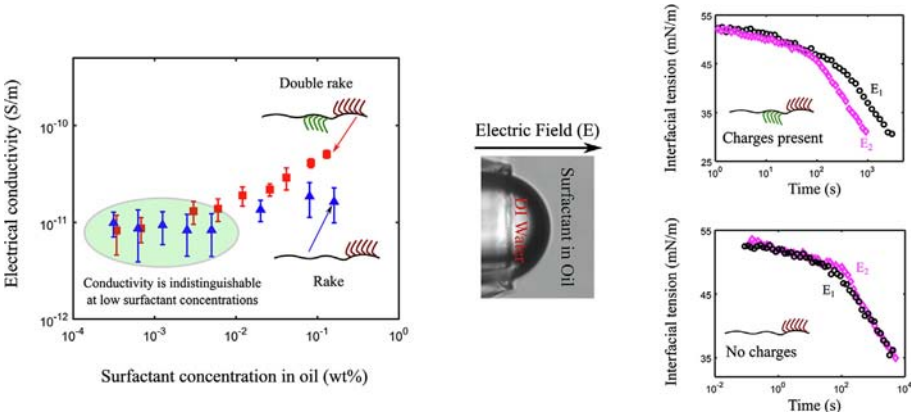

ARTICLE INFO

Article history:
Received 26 November 2019
Revised 2 January 2020
Accepted 3 January 2020
Available online 25 January 2020

Keywords:
Electric field
Surfactant transport
Adsorption
Oil-water interfaces
Interfacial tension
Charge carriers
Nonpolar media

ABSTRACT

Hypothesis: Electric fields enhance surfactant transport to oil-water interfaces when the surfactant forms charged aggregates in the oil phase. Hence, transport under electric fields could be used to detect charged surfactant aggregates in nonpolar media.

Experiments: Two surfactants with different architecture were dispersed in Isopar-M. The transport of surfactants to an oil-water interface under a constant electric field was quantified using a custom-built electrified microtensiometer platform. Electrical conductivity of the oil with surfactant concentration was also measured to determine the presence of charge carriers.

Findings: The charging mechanism of the oil phase, and field-enhanced transport was different for the two surfactants. At low concentrations where the electrical conductivity of the surfactants is indistinguishable, dynamic interfacial tension measurements under electric fields can ascertain the presence of charge carriers in Isopar-M. The transport of ionic surfactants in the aqueous phase was unaffected by the field, confirming that the field-enhanced transport of oil-phase surfactants is due to electrophoresis of charge carriers. Moreover, the equilibrium interfacial tension was not found to change under an electric field, suggesting the adsorption isotherm is independent of the field strength. We demonstrate that dynamic interfacial tension measurements under electric fields is a sensitive technique to detect charge carriers in nonpolar fluids.

* Corresponding author.
E-mail address: lwalker@andrew.cmu.edu (L.M. Walker).

https://doi.org/10.1016/j.jcis.2020.01.081
0021-9797/

1. Introduction

Control and characterization of the transport of surfactants to fluid-fluid interfaces is a key aspect to formulation design. In the absence of external fields, the transport and adsorption of a surfactant to an interface follows two simultaneous transport processes [1–4]. Surfactant molecules near the interface undergo adsorption and desorption from the bulk to the interface. This reduces the local surfactant concentration near the interface, establishing a concentration gradient across the bulk phases. Surfactant molecules diffuse from the bulk to the interface due to this concentration gradient. For an initially clean interface, the interfacial tension decreases on surfactant adsorption from the pure fluid-fluid interfacial tension, and relaxes to an equilibrium. The rate of surfactant transport is measured by the dynamic interfacial tension, and depends on the bulk concentration, isotherm, surfactant architecture and the geometry of the interface [3,5–8]. For a given system and geometry, it has been shown that the transport can be controlled using bulk convection [9–11], demonstrating the utility of external fields.

In nonpolar liquids, like oils, the addition of surfactants has been shown to increase the electrical conductivity, even when the surfactant is nonionic [12–18]. This is explained by the formation and stabilization of charged species due to the amphiphilic nature of the surfactants. The origin of charge is thought to be reverse micelles, with water trapped in the core of the micelle and surrounded by the polar head groups of the surfactant. Two neutral micelles undergo random collisions due to Brownian motion and exchange an ion (usually identified as a proton), producing two oppositely charged micelles. This mechanism is known as disproportionation of charge [15–21]. Another proposed mechanism for the origin of charge is the steric stabilization of ionizable impurities in oils by surfactant aggregates [13,22]. If the added surfactant is ionic, charges may arise due to partial dissociation of the surfactant [14,19]. While the exact origin and constituents of charge is still debated, we have recently shown that the transport of charge-forming surfactant aggregates in oil can be precisely manipulated using an external electric field [23].

A knowledge of the concentration of the charged species as a function of the added surfactant concentration is used to determine the charging mechanism in nonpolar media [18]. This is important in electrophoretic display technology [17,24], neutralizing streaming currents to prevent sparks and explosions in oil transport [25], and preventing soot formation in internal combustion engines [26]. Charge carrier concentration is usually determined by measuring the electrical conductivity of the nonpolar solvent as a function of surfactant concentration. The conductivity depends on the size and concentration of the charged species. Hence, by measuring the size through dynamic light scattering (DLS) [16,18] experiments, the concentration of charge carriers in the nonpolar phase can be estimated. However, most commercial surfactants are polydisperse, and light scattering experiments detect aggregates of all sizes. Significant errors can arise if the mean size of the aggregates is used to estimate the concentration of charge carriers [18]. As an alternate approach, electrochemical spectroscopy techniques can be used to measure the Debye length and relate it to the ionic strength of the solution [18,27]. However, the adsorption of charged species to the electrodes complicates the analysis of the results [18]. Measurements of electrical conductivity is widely used to detect the presence of charged species in oils. Commercially available non-aqueous conductivity meters employed for this purpose can measure conductivity $> 10^{-11}$ S/m. This puts a lower limit to the surfactant concentrations that can be studied for the presence of charge carriers [19,22]. Developing a more sensitive technique to detect charged species in oils, particularly at low surfactant concentrations can help understand charging in nonpolar media.

Recently, using a custom-built electrified capillary microtensiometer, we have shown that electric fields can be used to manipulate surfactant transport from bulk oil phases to oil-water interfaces, when the surfactant forms charged aggregates [23]. In nonpolar fluids, the aggregation of surfactant molecules may occur over a range of surfactant concentrations, rather than at a distinct critical micellar concentration (CMC) [16,28–31]. The tendency of the formed aggregates to acquire charge depends on the solvent in which the surfactant is dispersed [19], and size of the aggregates [15,19], which in turn is a function of surfactant architecture [32–34]. In the previous work, we had dispersed two different surfactants in two different oils, and measured the interfacial tension as a function of time, i.e., the dynamic interfacial tension, to establish electric fields as a tool to manipulate surfactant transport in oils [23]. Here, we use surfactants having different structures and charging behavior in the same nonpolar medium to determine if dynamic interfacial tension measurements under electric fields can be used to distinguish surfactants having different charging mechanisms.

In the present work, two surfactants with different architecture are dispersed in an alkane mixture, and the transport to an oil-water interface measured under different electric fields. The electrical conductivity of the oil is measured as a function of the surfactant concentration to determine the presence of charged species. The results are compared to our previous study on the transport of a different surfactant in the same oil [23]. Next, the transport of an ionic surfactant from the aqueous phase to the oil-water interface is measured under electric fields. Finally, the effect of electric fields on the equilibrium interfacial tension is established. We provide further evidence that the coupling between surfactant transport and electric fields occurs due to electrophoresis of charged species. Measurement of the dynamic interfacial tension of oil-water interfaces is a sensitive tool to detect charged species in oils, particularly at low surfactant concentrations, and holds promise in understanding charging in nonpolar media. In Section 2, we enlist the materials used and describe in detail the experimental platform to perform the measurements. In Section 3, we discuss the results of this work. In Section 4, we provide the conclusions of our work.

2. Materials and methods

2.1. Materials

Isopar-M, an alkane mixture of dodecane and tridecane is obtained from Exxon Mobil (Houston, TX) and used as received. Two surfactants having a rake (R-M) and a double rake (DR-L) morphology are obtained from the Dow Chemical Company (Midland, MI) and dispersed in the oil phase. Both these surfactants are silicone polyether surfactants and have a polyethylene glycol (PEG) functionality. The DR-L surfactant has an additional functionality of a dodecyl group. The structure of the two surfactants is shown in Fig. 1, along with the structure of a poly-isobutylene succinimde (OLOA 11000) surfactant for comparison to our previous work [23]. The exact molecular weight of the two rake surfactants was not known, but reported by the supplier to be 2–5 kDa and 4–15 kDa for the R-M and DR-L surfactants, respectively. Hence, surfactant concentrations were reported as wt% in this work. Stock solutions of 0.32 wt% R-M and 0.25 wt% DR-L were prepared in Isopar-M, which were then diluted to different concentrations for the experiments. In addition, 100 cSt silicone oil was purchased from Gelest, Inc. For the aqueous phase, deionized (DI) water was taken from a Barnstead UV Ultrapure II purification system (resistivity of 18.2

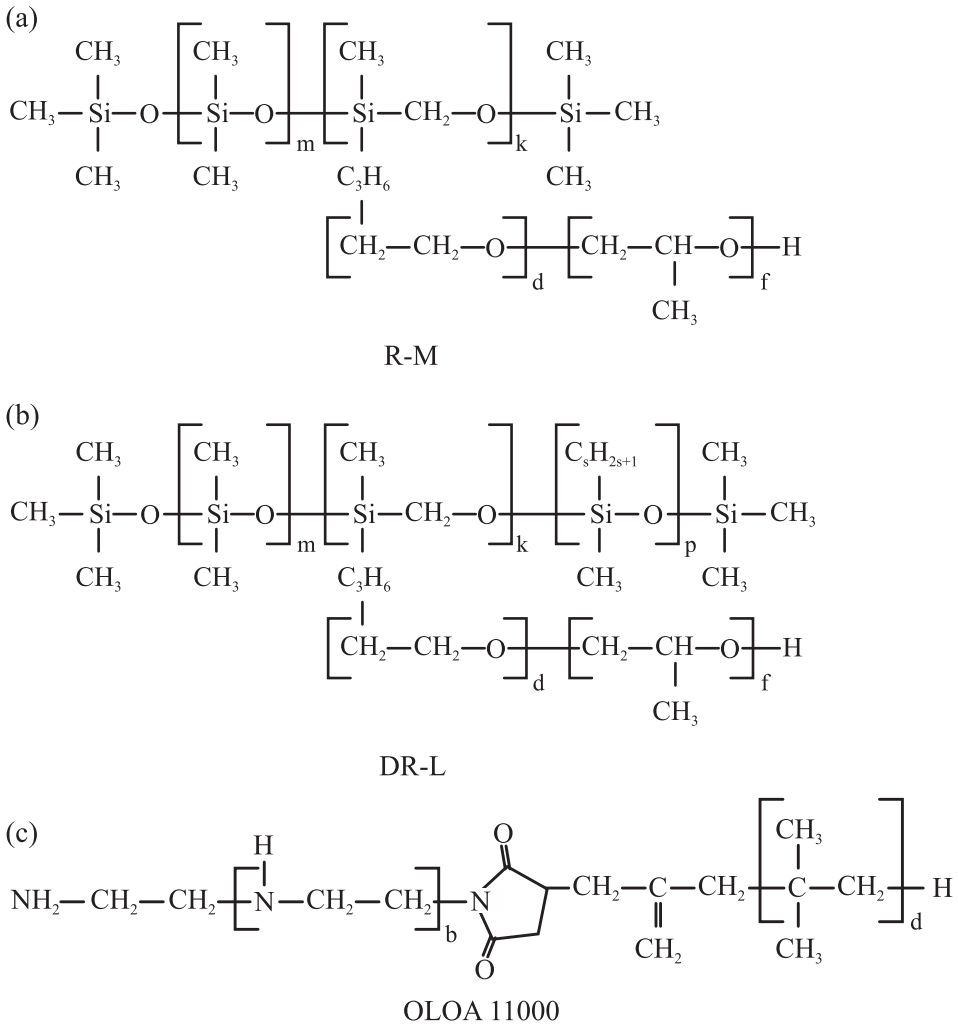

Fig. 1. Structure of (a) R-M (rake morphology), (b) DR-L (double rake morphology) and (c) OLOA 11000. The structures of the rake surfactants were provided by the supplier and that of OLOA 11000 was taken from Ref. [17].

MΩ cm). The ionic surfactant cetyltrimethylammonium bromide (CTAB) was purchased from Sigma–Aldrich (St. Louis, MO) at 99% purity, and dissolved in the aqueous phase at a concentration of 3.64×10^{-4} wt% (10 μM), along with 5.84×10^{-2} wt% (10 mM) sodium chloride. The critical micellar concentration (CMC) was reported by the supplier to be $3.28–3.64 \times 10^{-2}$ wt% (0.9–1 mM) in water, so the concentration used was below the CMC.

2.2. Microtensiometer under electric fields

The experimental setup resembles the microtensiometer platform, developed by Alvarez et al. [6], and is an electrified version of the same. The schematic of the equipment is shown in Fig. 2, with gravity pointing into the plane of the paper. The device consists of a cell with a rectangular cross-section (25 mm × 20 mm), machined out of Delrin ®. The cell is 40 mm deep, and is filled with the oil phase fluid. There are two ports drilled on opposite walls of the cell. The ports are designed to be at the same height, although machining inaccuracy can result in a height difference of around 10 μm. This translates to a hydrostatic pressure difference of 0.08 Pa, which is nearly $\mathcal{O}\left(10^{-5}\right)$ smaller than the capillary pressure, hence is negligible. A glass capillary containing the aqueous phase fluid is inserted through one of the ports, and the other port is connected to one end of a differential pressure transducer (Omega Engineering, PX409-001DWU5V). The other end of the pressure transducer is connected to the end of the glass capillary using polyethylene tubing having an internal diameter of 1 mm. For this study, the glass capillaries were pulled to diameters between 75 and 80 μm, using a PMP-102 micropipette puller (Micro Data Instrument, Inc.). Capillaries used for pulling were purchased from World Precision Instruments, Inc. (Sarasota, FL), and have an internal diameter of 0.75 mm, and an external diameter of 1 mm.

An interface between the oil and aqueous phase fluids is pinned at the tip of the capillary using a constant pressure head. This pressure head is generated using a water column attached to the capillary through the “normally open” port of a three-way solenoid valve, using polyethylene tubing (internal diameter of 1 mm). A high pressure head generated using a taller water column (≈ 35 cm) is connected to the “normally closed” port of the solenoid valve. A new interface is generated by pulsing the pressure head behind the capillary phase fluid and ejecting a drop. The transverse walls have glass windows, which enable viewing the interface. The interface was imaged using a Labview subroutine, with a camera (Point Grey Grasshopper) attached to a Nikon microscope objective lens (20×). The captured image was analyzed *in situ* by fitting a circle to the interface. The National Instruments Vision toolbox was used for detecting the interface and fitting a radius.

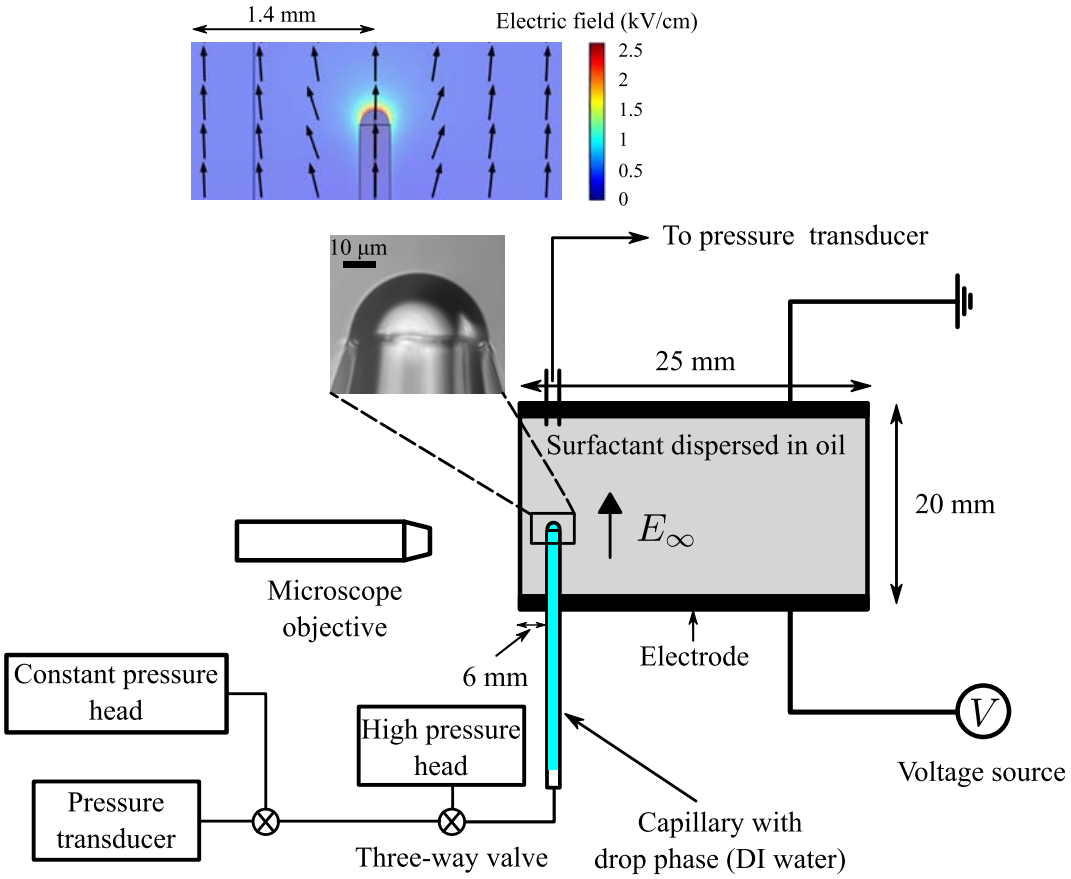

Fig. 2. Schematic of the experimental setup. Gravity points into the plane of the paper. Top left inset shows COMSOL simulations of electric field lines around a capillary of diameter 70 μm.

The walls with ports for the capillary and the pressure transducer are also provided with slots for the insertion of stainless steel electrodes. Voltages in the range 0.1–0.8 kV were applied using a high voltage source (Gamma High Voltage), setting electric fields $\sim 0.05 - 0.4$ kV/cm across the cell, along the axis of the capillary. Switching the voltage on and off did not cause any fluctuations in the signals obtained from the pressure transducer, verifying that this range of voltage does not interfere with the electric signals of the pressure transducer. An electric field larger than 0.4 kV/cm caused the contact angle of the interface with the glass capillary to change due to electrowetting [35]. Thus, fields larger than 0.4 kV/cm were not studied. COMSOL simulations were used to predict the distribution of electric field lines in the cell around the capillary. The simulations predict that electric field lines are not affected by the walls of the cell when the gap between the wall and capillary is more than 20 capillary radii. To ensure that the capillary is within the field of view of the camera, and the electric field lines are unaffected by the wall, it was placed at a distance of 6 mm (75 capillary radii) from the wall near the camera.

2.3. Interfacial tension measurements

Surfactant transport is quantified by the dynamic interfacial tension, γ, of the interface. This is obtained from the instantaneous normal stress balance across the interface, which can be written as

$$\Delta\tilde{P}(t) = \frac{2\gamma(t)}{\tilde{R}(t)} - \Delta\tilde{T}_E, \tag{1}$$

where $\Delta\tilde{P}$ is the Laplace pressure, $\tilde{R}$ is the radius of curvature of the interface, and $\Delta\tilde{T}_E$ is the jump in normal electric stresses at the interface, measured as the difference between electric stresses outside and inside the interface. The superscript, $\sim$, denotes a dimensional quantity. The electric stresses scale as $\varepsilon_o E_\infty^2$, where ε_o is the permittivity of the reservoir phase fluid, and E_∞ is the applied electric field; and is used to non-dimensionalize stresses. Scaling length with the capillary radius, R_c, and the Laplace pressure using the maximum capillary pressure (γ/R_c), the non-dimensional form of the normal stress balance across the interface reduces to

$$\Delta P(t) = \frac{2}{R(t)} - Ca_E \Delta T_E, \tag{2}$$

where $Ca_E = \varepsilon_o R_c E_\infty^2/\gamma$ is the electric capillary number, which is a ratio of the electric stresses to the capillary pressure, and the terms without the superscript denote equivalent dimensionless quantities. Here, R and $\Delta T_E \sim \mathcal{O}(1)$, and for the electric field strengths used in this work, $Ca_E < \mathcal{O}\left(10^{-4}\right)$. Thus, electric stresses were ignored from the normal stress balance, and the dynamic interfacial tension was calculated using the Young-Laplace equation,

$$\gamma(t) = \frac{1}{2}\Delta\tilde{P}(t) \times \tilde{R}(t). \tag{3}$$

The small value of the electric capillary number also ensures that the electric field does not deform the interface, or cause any interfacial instability [36–39].

To verify that the scaling is correct and electric stresses can be ignored from the normal stress balance, the interfacial tension of oil-water interfaces with no added surfactant was measured under the highest electric field chosen in this study (0.4 kV/cm), and compared to the interfacial tension under no applied field. The result is shown in Fig. 3, where the interfacial tension was measured for at

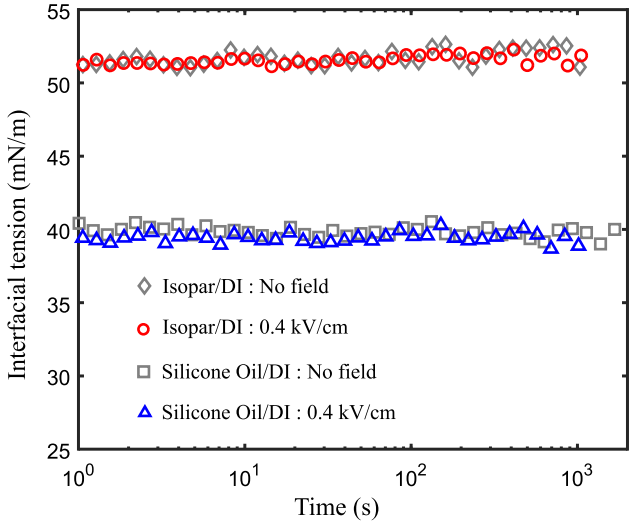

Fig. 3. Interfacial tension of Isopar-DI water and 100 cSt silicone oil-DI water under no field, and under 0.4 kV/cm.

least 1000 s. The interfacial tension of Isopar-DI water was measured to be 52 ± 0.6 mN/m under no electric field, and 51.7 ± 0.3 under 0.4 kV/cm; and that of 100 cSt silicone oil-DI water interface was measured to be 39.9 ± 0.4 mN/m under no field, and 39.5 ± 0.4 mN/m under 0.4 kV/cm. The measured values are in agreement with previously reported values [8,40]. For experiments under electric fields, a new interface was formed while the field was switched on, and the interfacial tension was measured using (3). Notably, the difference between the measured interfacial tension under zero field and the largest field applied is less than 1 mN/m, which is the error in interfacial tension measurement of the technique [6,23]. The sudden application of the electric field across an interface formed under zero field did not change the interfacial tension. This shows that the interfacial tension of Isopar-DI water and silicone oil-DI water interfaces with no added surfactant does not change under electric fields of up to 0.4 kV/cm. A similar observation was recently made for xylene-water interfaces under electric fields of up to 0.82 kV/cm [41].

When surfactants are present, the interfacial tension of a new interface starts at the value of clean oil-water interfacial tension in the absence of surfactants, which is nearly 52 mN/m for an Isopar-DI water interface. As the surfactant adsorbs to the interface, the interfacial tension decreases and eventually relaxes to an equilibrium. Similar to our previous study, the interface was deduced to reach equilibrium when the interfacial tension does not change by more than 1 mN/m for a period of at least 1000 s [23]. During the experiments, data was collected at every millisecond; however, for clarity, we first smooth the data using a piecewise cubic Hermite interpolating polynomial, and show 50 data points spaced equally on a logarithmic scale in all the figures. For a given surfactant concentration, the pressure head was held constant at the same value, and changes in the interfacial tension occurred due to a decrease in the radius of curvature of the interface. This ensured that the initial condition for experiments conducted under different electric fields at a fixed surfactant concentration was the same.

3. Results and discussion

3.1. Transport of oil-soluble surfactants

The transport of the rake (R-M) and double rake (DR-L) surfactants was measured to the Isopar-DI water interface, and is shown in Fig. 4. For comparison, the transport of 4.8×10^{-4} wt% OLOA to the Isopar-DI water interface, which was measured in our previous study, is also shown [23]. This data is reproduced from Fig. 2(a) of

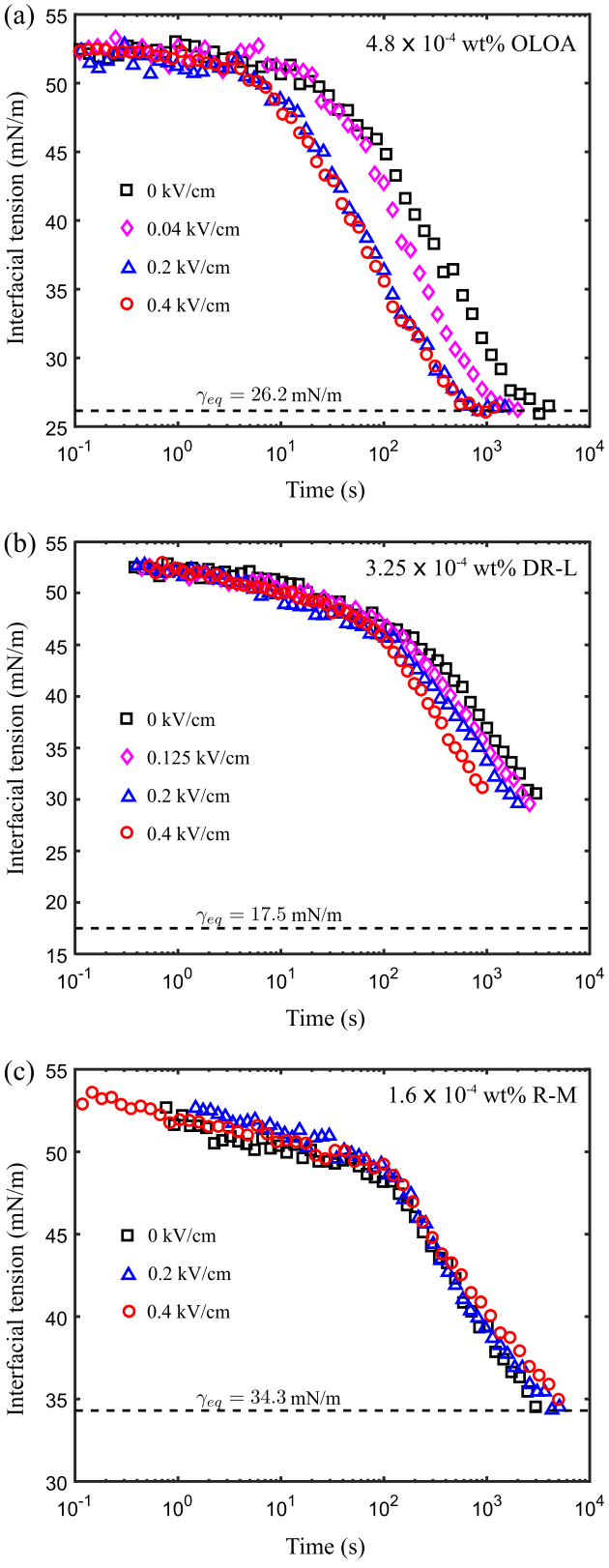

Fig. 4. Dynamic interfacial tension of (a) 4.8×10^{-4} wt% OLOA 11000, (b) 3.25×10^{-4} wt% DR-L and (c) 1.6×10^{-4} wt% R-M in Isopar-M. The dashed lines represent the equilibrium interfacial tension.

that paper, and corresponds to the dynamic interfacial tension of 4 μM OLOA [23]. At this concentration of OLOA, the interfacial tension of the Isopar-DI water interfaces relaxes to a steady state of 26.3 ± 0.3 mN/m. The interface reaches steady state faster as the strength of the applied electric field increases. Under a field of 0.4 kV/cm, the steady state is reached nearly four times faster than under no applied field. The steady state interfacial tension is statistically the same under all applied fields, as indicated by the dashed line. The effect of electric field on surfactant transport is more prominent at smaller values of the electric field. The dynamic interfacial tension curves under 0.2 and 0.4 kV/cm nearly overlap each other, although slightly faster dynamics was observed under 0.4 kV/cm. Clearly, electric fields enhance the transport of OLOA to the Isopar-water interface.

The dynamic interfacial tension of 3.25×10^{-4} wt% DR-L is shown in Fig. 4(b) under different electric fields. For this system, the pressure head was initially maintained at $\tilde{1}500$ Pa. A smaller pressure head generated a very flat interface ($\tilde{R}(t)/R_c > 2$) during the initial few minutes of the dynamics, which results in a large error in the measurement of the radius of curvature of the interface. The equilibrium interfacial tension at this concentration is 17.5 ± 0.6 mN/m. In the figure, the dynamic interfacial tension data is shown until an interfacial tension of around 30 mN/m. At this value, the radius of curvature of the interface is very close to the radius of the capillary, and the interface gets ejected from the capillary tip if the pressure head is not reduced. Once this interfacial tension was reached, the pressure head was reduced to 750 Pa, and data was collected until the system relaxed to equilibrium. During the first 100 s, the transport of DR-L was only slightly enhanced by the electric field. Beyond this time, there is clearly an enhancement of the transport under electric fields. Under a field of 0.4 kV/cm, the interfacial tension reduced to 35 mN/m nearly three times faster than under no applied electric field. This observation is similar to the electric field-enhanced transport of OLOA 11000 to an Isopar-DI water interface [23].

In contrast, the transport of R-M at a concentration of 1.6×10^{-4} wt% was not affected by the electric field (Fig. 4(c)). The dynamic interfacial tension curves obtained under all electric fields nearly overlapped each other. The equilibrium interfacial tension at this concentration was measured to be 34.3 ± 0.8 mN/m. The equilibrium was found to be nearly independent of the electric field, similar to measurements for the transport of OLOA 11000 and DR-L to the Isopar-DI water interface (Fig. 4 (a) and (b)).

To further illustrate the effect of electric field on surfactant transport, the time taken for the interfacial tension to drop to half the interfacial tension of pure Isopar-DI water and the steady state interfacial tension at a given surfactant concentration, $t_{1/2}$, was plotted as a function of electric field. At the surfactant concentrations shown in Fig. 4, this interfacial tension corresponds to a value of 35 mN/m for OLOA, 36.5 mN/m for DR-L and 43 mN/m for R-M. The result, shown in Fig. 5, clearly demonstrates that electric fields enhance the transport of OLOA and DR-L to the Isopar-water interface, but does not affect the transport of R-M at 1.6×10^{-4} wt%. A one-way ANOVA test was performed to establish the statistical significance of this conclusion [42]. The results are shown in Table 1. This tests the null hypothesis that $t_{1/2}$ does not depend on the electric field strength. The F statistic here is defined as the ratio of variation between the mean $t_{1/2}$ under different field strengths to the variation in $t_{1/2}$ for a given electric field. The large values of the F statistic for OLOA and DR-L, along with the small p-value (< 0.05) for these surfactants confirms that the null hypothesis is rejected, and the result is statistically significant. For the R-M surfactant, the F statistic is small (< 1), and the p-value is large (> 0.05), which implies that the mean $t_{1/2}$ is statistically the same under different electric fields. For the data taken under an electric field, the time scale, $t_{1/2}$ for OLOA transport shows a power-law scaling, with an exponent of 0.4, as shown by the dashed line in Fig. 5. On the other hand, for DR-L, $t_{1/2}$ decreases linearly as the applied field strength increases. An explanation for the observed trend in the time scale would require a detailed analysis of the adsorption isotherm, and is left as future work.

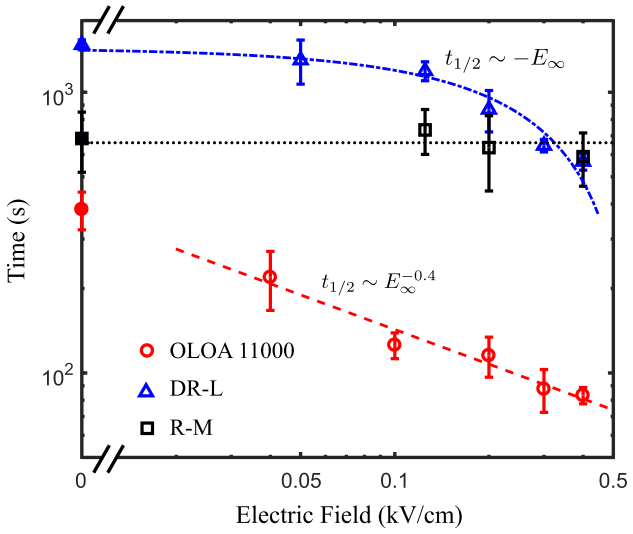

Fig. 5. Time required for the interfacial tension to drop to half the interfacial tension of pure Isopar-DI water and the steady state interfacial tension. The filled symbols on the left show the time under no applied field. The dashed and dash-dotted lines are best fit lines to the data for OLOA and DR-L, respectively. The dotted horizontal line shows the time is independent of the applied field strength for R-M.

Table 1
Results of a one-way ANOVA test for the null hypothesis that the time to reach half the interfacial tension of pure Isopar-DI water and the steady state interfacial tension, $t_{1/2}$, does not change under an electric field.

Surfactant	F statistic	p value
OLOA 11000	33.39	1×10^{-8}
DR-L	27.46	3.6×10^{-6}
R-M	0.64	0.603

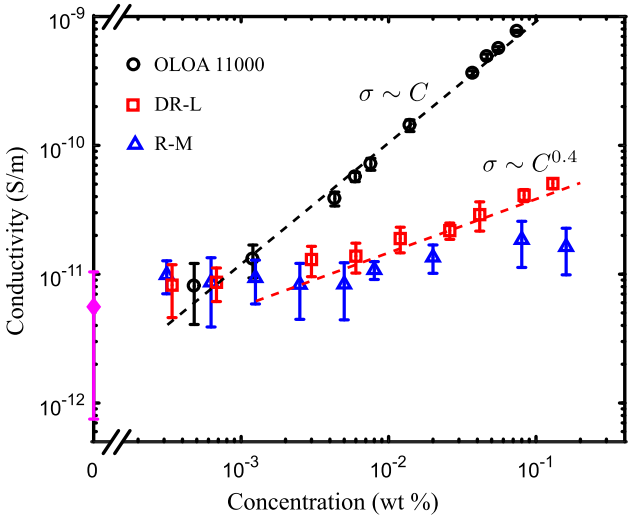

Fig. 6. Electrical conductivity of Isopar-M as a function of concentration of added surfactant. Symbols denote experimental measurements, and the dashed lines show the trend in conductivity with surfactant concentration. The filled symbol on the left axis denotes the conductivity of Isopar-M with no added surfactant.

The electrical conductivity of Isopar-M as a function of the concentration of the two rake surfactants was measured, and is shown in Fig. 6, along with the conductivity for OLOA in Isopar-M to compare to our previous work [23]. The conductivity was measured using a nonaqueous conductivity probe (DT 700, Dispersion Technology). This instrument has a resolution of 10^{-13} S/m; however considerable noise was observed in the data at low surfactant concentrations ($< 10^{-3}$ wt%), where the measured average conductivity was $< 10^{-11}$ S/m and the standard deviation was 25–50% the average value. The conductivity at these low concentrations is comparable to the measured conductivity of Isopar-M with no added surfactant, which is shown by the filled symbol on the left axis in Fig. 6. At higher concentrations, the electrical conductivity of Isopar-M increases linearly with the concentration of OLOA, both above and below the reported CMC in alkanes and alkane mixtures having a composition similar to Isopar-M (5×10^{-3}–1.68×10^{-2} wt%) [20,21]; and nearly as the square root of the concentration of DR-L. There is no significant increase in the conductivity with addition of R-M. The conductivity increases by factor of 2 at a concentration of around 10^{-2} wt%, however, further addition of surfactant did not systematically increase the conductivity.

An increase in electrical conductivity with surfactant concentration is indicative of the presence of charged species, which is attributed to water-swollen inverse surfactant micelles, or ionic impurities in oils sterically stabilized by surfactants [13–15,17–22]. It has been suggested that in nonpolar liquids, a distinct CMC may not exist, and aggregation of surfactant molecules into micelles in nonpolar solvents may occur either at a distinct concentration, or gradually over a range of concentrations, depending on the polarity of the surfactant molecule [28–31]. A linear increase in conductivity with concentration can be explained by disproportionation of charge by the collision of two neutral aggregates - inverse micelles, or complexes of ionizable impurities with surfactant molecules [15,17–22]. An increase in conductivity as the square root of concentration is attributed to partial dissociation of ion pairs, and has been observed with dioctyl sodium sulfosuccinate (NaAOT) in hexadecane at concentrations below the CMC [14]. The structure of DR-L does not suggest any ionizable group. Further, conductivity measurements and preliminary experiments done with dynamic light scattering (DLS) did not reveal any distinct CMC. Hence, instead of determining the constituents of charges, we conclude that addition of both OLOA 11000 and DR-L to Isopar-M gives rise to charged species, most likely by different charging mechanisms. An electric field will act on these species and give rise to an electrophoretic transport, in addition to the diffusive transport of the surfactant from the bulk to the interface. We have shown previously that even under the smallest electric field used in the experiments, the electrophoretic transport of the charged surfactant complexes occur at least an order of magnitude faster than the diffusive transport [23]. This manifests as an enhanced transport, observed in the dynamic interfacial tension measurement for OLOA and DR-L (Fig. 4 (a) and (b)). The difference in the observed scaling of $t_{1/2}$ with E_∞ for these two surfactants could also be attributed to their different charging mechanisms in Isopar-M, as evidenced by the conductivity data (Fig. 6).

Notably, the electrical conductivity of Isopar-M at the concentrations of the three surfactants studied in Fig. 4 is not statistically different from each other, or from the conductivity of Isopar-M with no added surfactant. As such, a measurement of the conductivity alone at these lower concentrations would lead to a conclusion of the absence of charge carriers. The three surfactants, however, show a different response under an electric field. In particular, the field-enhanced transport of OLOA and DR-L are indicative of the presence of charged species which respond to the applied field. This demonstrates that at low surfactant concentrations, a measurement of the dynamic interfacial tension of oil-water interfaces under electric fields is a sensitive tool to detect the presence of charged species in oils.

The conductivity of Isopar-M increased by a factor of 2 with the addition of R-M at a concentration of around 10^{-2} wt%. Although there is no significant increase in conductivity with further increase in the concentration, the dynamic interfacial tension for both R-M and DR-L was measured around this concentration to check for field-enhanced surfactant transport. The results are shown in Fig. 7(a) for 1.3×10^{-2} wt% DR-L and Fig. 7(b) for 8×10^{-3} wt% R-M. For both these systems, the interfacial tension was observed to relax to values < 10 mN/m. At these low interfacial tensions, the constant pressure head, $\Delta\widetilde{P}$ needs to be reduced to nearly 400 Pa, which is around four times the accuracy of the pressure transducer. This compromises the accuracy of the measured interfacial tension. Consequently, an equilibrium interfacial tension was not measured at these concentrations. Instead, the dynamics of surfactant transport was probed till the interfacial tension reduced to around 20 mN/m for the DR-L system, and 17 mN/m for the R-M surfactant. The transport of both surfactants

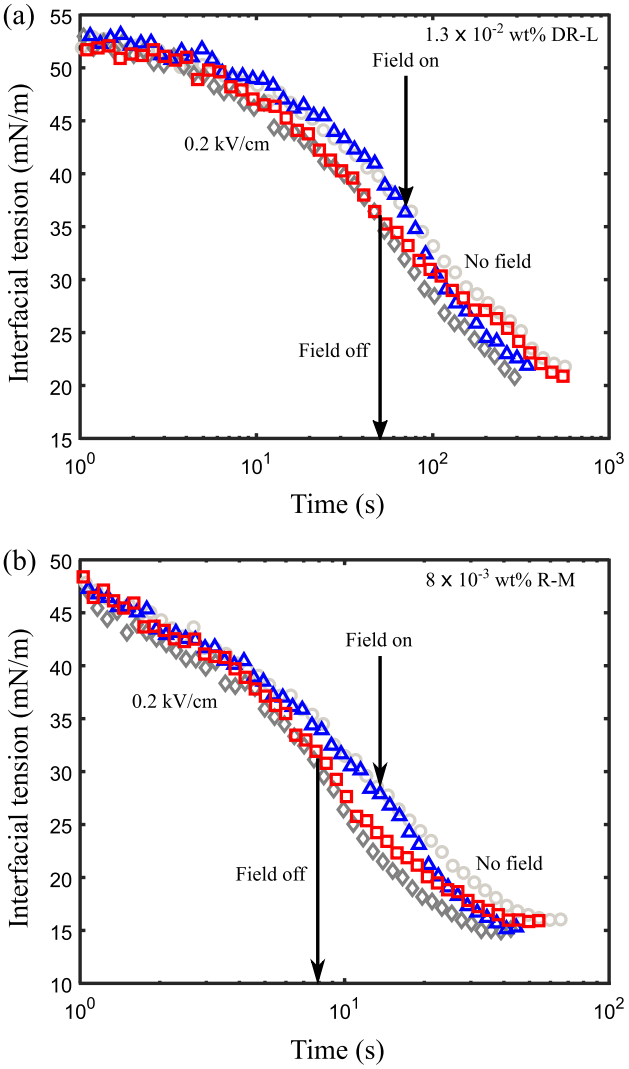

Fig. 7. Dynamic interfacial tension of (a) 1.3×10^{-2} wt % DR-L and (b) 8×10^{-3} wt % R-M in Isopar-M, performed under no field (○), 0.2 kV/cm (◇), no field to 0.2 kV/cm (△) and 0.2 kV/cm to no field (□). The arrows indicate the time when the field was switched on or off.

at the higher concentration was faster for all fields when compared to experiments performed at a lower concentration (Fig. 4). This is in agreement with previous observations of faster transport of surfactants from more concentrated bulk solutions, when the transport is in the diffusion limited regime [7,8]. Further, even under no applied field, the interfacial tension relaxed to the measured limits relatively fast, at around 600 s for DR-L and 80 s for R-M. Given the narrow range in time for the decrease in interfacial tension, rather than measuring the transport over a range of different electric field strengths, experiments were performed which started under no applied field. A field of 0.2 kV/cm was then applied at 70 s for DR-L and 15 s for R-M, analogous to experiments performed with OLOA in Isopar-M [23]. For both the surfactants, the transport dynamics changed instantaneously with the application of the field. The dynamic interfacial tension curve shifted from the curve obtained under no field throughout the experiment to the curve obtained under 0.2 kV/cm throughout the experiment. Another experiment was performed where the measurement was started under 0.2 kV/cm, with the field being switched off at 50 s for DR-L, and 8 s for R-M. Again, for both surfactants, the dynamics changed at the instant the field was switched off, and the dynamic interfacial tension curve shifted from the one obtained under 0.2 kV/cm throughout the experiment to the one obtained under no field throughout the experiment. For both DR-L and R-M, an electric field enhanced the transport at these higher concentrations.

The enhancement in transport of the DR-L surfactant at the higher concentration is expected, given a similar observation at a lower concentration. It can be explained by the electrophoresis of charge carriers under electric fields, the presence of which was indicated by the increase in Isopar-M conductivity with addition of DR-L (Fig. 6). On the contrary, the transport of R-M, which was not affected by electric fields at a lower concentration (1.6×10^{-4} wt%), was influenced at 8×10^{-3} wt%. A field-enhanced transport for R-M was also observed at an even higher concentration of 1.6×10^{-2} wt%, but is not shown here. The conductivity of Isopar-M remained relatively constant with increasing concentration of R-M, until around 10^{-2} wt%, where the conductivity almost doubled. This, coupled with the observation of a field-enhanced transport around a similar concentration suggests the presence of charged species, which most likely can be attributed to surfactant aggregates [13,15,19]. Although further addition of surfactant did not show a systematic increase in the conductivity, previous studies have shown that the aggregation of surfactants to micelles in nonpolar liquids can occur gradually over a range of concentrations, depending on the polarity of the surfactant [28,31]. The tendency of surfactant aggregates to acquire charge and give rise to conductivity was shown to depend on the size of the aggregates [15], which in turn depends on the surfactant architecture [32–34]. Thus, the formation of charge carriers, charging mechanism, and coupling of electric fields and surfactant transport in nonpolar liquids depends on the polarity and architecture of the surfactant molecule. The field-enhanced transport of R-M at a concentration $\geqslant 8 \times 10^{-3}$ wt % indicates that the surfactant forms charged complexes in Isopar-M at around this concentration. Below this concentration, the R-M surfactant does not contribute to charging of the oil phase. The transport of surfactants to oil-water interfaces can be precisely manipulated using electric fields at these concentrations where the surfactant forms charged aggregates.

We reiterate that the measurement of solely the electrical conductivity of Isopar-M doped with R-M would not detect charge carriers, especially at a concentration of 8×10^{-3} wt% because the conductivity till this concentration is not statistically different from the conductivity of Isopar-M with no added surfactant. Measurements of the dynamic interfacial tension for these low conductivity systems is a more sensitive technique to ascertain the presence of charge carriers, and detect changes in charge carrier concentration with the addition of small amounts of surfactant. It is still unclear how the concentration of charge carriers, or the charging mechanism can be determined from the dynamic interfacial tension data or the observed scaling of $t_{1/2}$ with E_∞ obtained from these experiments. Nevertheless, dynamic interfacial tension measurement under electric fields shows promise to understand charging in nonpolar media, particularly at low surfactant concentrations.

3.2. Transport of ionic surfactants in aqueous phase

Next, the transport of the cationic surfactant CTAB from the aqueous phase to the oil-water interface was studied under electric fields. A 3.64×10^{-4} wt% concentration of the surfactant was prepared in a solution of 5.84×10^{-2} wt% sodium chloride. Addition of salt reduces the electrostatic repulsion between surfactant headgroups, which increases the tendency of the surfactant to adsorb at the interface. The result is shown in Fig. 8. The interfacial tension relaxes to an equilibrium of 34.5 ± 0.7 mN/m, indicated by the dashed line. Evidently, the transport of the cationic CTAB does not depend on the electric field. The electrical conductivity of deionized water is nearly $\mathcal{O}\left(10^6\right)$ larger than Isopar-M. Adding salt further increases the conductivity. Due to the large difference in conductivity, the aqueous phase can be considered to be a conducting fluid. The electric field inside the aqueous phase scales as the ratio of conductivity of the oil to aqueous phase, and is nearly zero [36]. Thus, although cationic surface active species are present in the aqueous phase, there is no electric field to drive the charged species to the interface. As a result, the transport of surfactants from an aqueous phase to oil-water interfaces is not affected by an electric field. This further verifies that the enhancement in transport observed for oil-phase surfactants is caused by the electrophoretic motion of charge carriers.

3.3. Equilibrium interfacial tension

Finally, the effect of electric field on the equilibrium interfacial tension at the Isopar-DI water interface was measured. The result is shown in Fig. 9 for OLOA 11000, DR-L, R-M and CTAB at a given concentration for electric fields of up to 0.4 kV/cm. A one-way

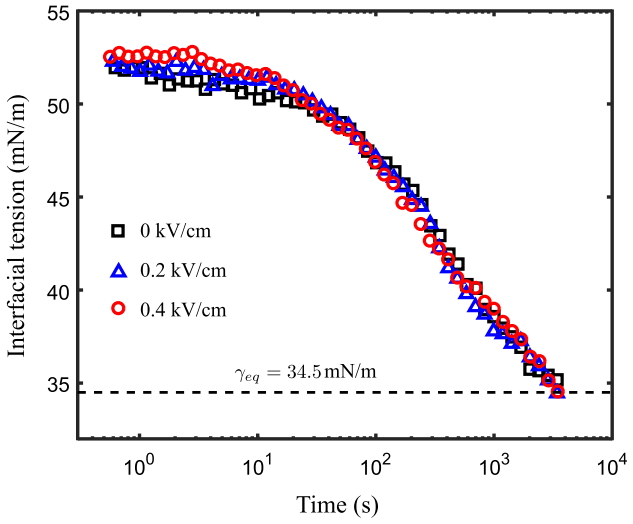

Fig. 8. Dynamic interfacial tension of 3.64×10^{-4} wt% CTAB in 5.84×10^{-2} wt% sodium chloride. The dashed line represents the equilibrium interfacial tension.

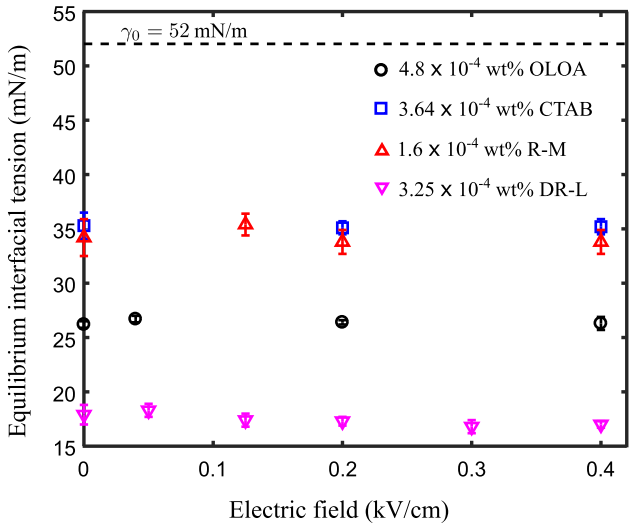

Fig. 9. Equilibrium interfacial tension of the surfactants plotted as a function of the electric field strength. The dashed line denotes the interfacial tension of an Isopar-DI water interface in the absence of added surfactant.

Table 2
Results of a one-way ANOVA test for the null hypothesis that the mean equilibrium interfacial tension does not change under electric field.

Surfactant	F statistic	p value
OLOA 11000	0.65	0.5823
DR-L	2.17	0.1265
R-M	0.95	0.4627
CTAB	0.38	0.7

ANOVA test (Table 2) shows that the value of the F statistic is $\mathcal{O}(1)$, and the p value is > 0.05 for all four surfactants. Hence, it follows that the equilibrium interfacial tension does not change under an applied electric field of up to 0.4 kV/cm. Although a full adsorption isotherm was not measured, we conclude that the isotherm parameters do not change under electric fields.

4. Conclusions

The transport of surfactants which form charged aggregates in nonpolar liquids is enhanced to oil-water interfaces under electric fields. The accelerated transport occurs due to the electrophoretic motion of the charged species under electric fields. The formation of charge carriers and the charging mechanism depends on the concentration, polarity and architecture of the surfactant molecules [28–31]. Two surfactants with different architecture were dispersed in Isopar-M, and the transport was measured to an Isopar-water interface. The DR-L surfactant, having a double rake morphology showed a field-driven transport at both concentrations studied, analogous to the field-enhanced transport of OLOA reported previously [23]. The R-M surfactant, with a rake morphology showed a field-enhanced transport at the higher concentration studied, and a field-independent transport at the lower concentration, which indicates that this surfactant forms charged aggregates in Isopar-M above a certain concentration. The transport of ionic surfactants in the aqueous phase was not influenced by an electric field. The electric field in the aqueous phase is nearly zero due to the large electrical conductivity of the aqueous phase compared to the oil phase. This further verifies that the field-enhanced transport for the oil-phase surfactants is due to electrophoresis of charged species. The equilibrium interfacial tension did not change on the application of an electric field, suggesting the surfactant adsorption isotherm is not a function of the electric field.

At low surfactant concentrations, the electrical conductivity of oils is very small. The sole measurement of the electrical conductivity could erroneously suggest the absence of charged species in the nonpolar phase. We show that at these low concentrations, measurement of the dynamic interfacial tension of an oil-water interface under electric fields is a sensitive tool to detect the presence of charge carriers, which would go unnoticed by conductivity measurements [19,22]. Notably, surfactants with different charging mechanisms show a different dynamic response to the electric field. It remains to be determined how the concentration of charge carriers, or the specific charging mechanism can be determined from the dynamic interfacial tension data. Measuring the adsorption isotherm to obtain pertinent length scales for surfactant transport, and a rigorous analysis of the time scale to reach half the clean interfacial tension and equilibrium interfacial tension value might offer useful information. The charging of nonpolar phases at high surfactant concentrations, where electrical conductivity can be confidently measured is relatively well explored [12–19,22]. We demonstrate that dynamic interfacial tension measurements under electric fields is a promising, sensitive technique to understand charging in nonpolar media, particularly at low surfactant concentrations.

Electric fields also show promise as a robust tool to selectively manipulate surfactant transport to oil-water interfaces. For example, in a dispersion containing both DR-L and R-M, the transport of DR-L can be preferentially enhanced by switching on an electric field, provided the concentration of R-M is low. A careful molecular design of surfactant to control the range of concentrations where the surfactants form aggregates and acquire charge will enable precise and selective manipulation of the transport of oil-soluble surfactants using electric fields. Moreover, electric fields selectively act on surfactants in the oil phase. Hence, unlike other parameters to control surfactant transport [3,5–11], electric fields could be employed to preferentially transport oil-soluble surfactants to oil-water interfaces in applications where surfactants from both the aqueous and oil phase are adsorbing to the interface. The application of electric fields to surfactants dispersed in oil provides us with an opportunity to precisely and selectively manipulate transport, and further understand charging in nonpolar media.

Declaration of Competing Interest

The authors declare that they have no known competing financial interests or personal relationships that could have appeared to influence the work reported in this paper.

Acknowledgements

Funding for this work was provided by the National Science Foundation through Grant No. CBET-1804548. RS acknowledges the funding provided by the John E. Swearingen Graduate fellowship, and the Bushnell Fellowship.

References

[1] S.-Y. Lin, K. McKeigue, C. Maldarelli, Diffusion-controlled surfactant adsorption studied by pendant drop digitization, AIChE J. 36 (12) (1990) 1785–1795.
[2] R. Pan, J. Green, C. Maldarelli, Theory and experiment on the measurement of kinetic rate constants for surfactant exchange at an air/water interface, J. Colloid Interf. Sci. 205 (2) (1998) 213–230.
[3] J. Eastoe, J. Dalton, Dynamic surface tension and adsorption mechanisms of surfactants at the air–water interface, Adv. Colloid Interfac. 85 (2–3) (2000) 103–144.
[4] F. Jin, R. Balasubramaniam, K.J. Stebe, Surfactant adsorption to spherical particles: the intrinsic length scale governing the shift from diffusion to kinetic-controlled mass transfer, J. Adhes. 80 (9) (2004) 773–796.

[5] S.-Y. Lin, R.-Y. Tsay, L.-W. Lin, S.-I. Chen, Adsorption kinetics of $C_{12}E_8$ at the air-water interface: adsorption onto a clean interface, Langmuir 12 (26) (1996) 6530–6536.
[6] N.J. Alvarez, L.M. Walker, S.L. Anna, A microtensiometer to probe the effect of radius of curvature on surfactant transport to a spherical interface, Langmuir 26 (16) (2010) 13310–13319.
[7] N.J. Alvarez, L.M. Walker, S.L. Anna, Diffusion-limited adsorption to a spherical geometry: The impact of curvature and competitive time scales, Phys. Rev. E 82 (1) (2010) 011604.
[8] N.J. Alvarez, W. Lee, L.M. Walker, S.L. Anna, The effect of alkane tail length of CiE8 surfactants on transport to the silicone oil–water interface, J. Colloid Interf. Sci. 355 (1) (2011) 231–236.
[9] T. Svitova, M. Wetherbee, C. Radke, Dynamics of surfactant sorption at the air/water interface: continuous-flow tensiometry, J. Colloid Interf. Sci. 261 (1) (2003) 170–179.
[10] V. Fainerman, S. Lylyk, J.K. Ferri, R. Miller, H. Watzke, M. Leser, M. Michel, Adsorption kinetics of proteins at the solution/air interfaces with controlled bulk convection, Colloids Surf., A 282 (2006) 217–221.
[11] N.J. Alvarez, D.R. Vogus, L.M. Walker, S.L. Anna, Using bulk convection in a microtensiometer to approach kinetic-limited surfactant dynamics at fluid–fluid interfaces, J. Colloid Interf. Sci. 372 (1) (2012) 183–191.
[12] M.F. Hsu, E.R. Dufresne, D.A. Weitz, Charge stabilization in nonpolar solvents, Langmuir 21 (11) (2005) 4881–4887.
[13] A.S. Dukhin, P.J. Goetz, How non-ionic "electrically neutral" surfactants enhance electrical conductivity and ion stability in non-polar liquids, J. Electroanal. Chem. 588 (1) (2006) 44–50.
[14] S.K. Sainis, J.W. Merrill, E.R. Dufresne, Electrostatic interactions of colloidal particles at vanishing ionic strength, Langmuir 24 (23) (2008) 13334–13337.
[15] Q. Guo, V. Singh, S.H. Behrens, Electric charging in nonpolar liquids because of nonionizable surfactants, Langmuir 26 (5) (2009) 3203–3207.
[16] S. Poovarodom, J.C. Berg, Effect of particle and surfactant acid–base properties on charging of colloids in apolar media, J. Colloid Interf. Sci. 346 (2) (2010) 370–377.
[17] G.N. Smith, J. Eastoe, Controlling colloid charge in nonpolar liquids with surfactants, Phys. Chem. Chem. Phys. 15 (2) (2013) 424–439.
[18] B.A. Yezer, A.S. Khair, P.J. Sides, D.C. Prieve, Use of electrochemical impedance spectroscopy to determine double-layer capacitance in doped nonpolar liquids, J. Colloid Interf. Sci. 449 (2015) 2–12.
[19] D.C. Prieve, B.A. Yezer, A.S. Khair, P.J. Sides, J.W. Schneider, Formation of charge carriers in liquids, Adv. Colloid Interfac. 244 (2017) 21–35.
[20] F. Strubbe, A.R. Verschueren, L.J. Schlangen, F. Beunis, K. Neyts, Generation current of charged micelles in nonaqueous liquids: measurements and simulations, J. Colloid Interf. Sci. 300 (1) (2006) 396–403.
[21] M. Gacek, D. Bergsman, E. Michor, J.C. Berg, Effects of trace water on charging of silica particles dispersed in a nonpolar medium, Langmuir 28 (31) (2012) 11633–11638.
[22] A. Dukhin, S. Parlia, Ions, ion pairs and inverse micelles in non-polar media, Curr. Opin. Colloid Interface Sci. 18 (2) (2013) 93–115.
[23] R. Sengupta, A.S. Khair, L.M. Walker, Electric fields enable tunable surfactant transport to microscale fluid interfaces, Phys. Rev. E 100 (2) (2019) 023114.
[24] Y. Chen, Flexible active-matrix electronic ink display; may 8, 2003; 136, Nature 423 (2003) 136.
[25] I.D. Morrison, Electrical charges in nonaqueous media, Colloids Surf., A 71 (1) (1993) 1–37.
[26] A. Klinkenberg, J.L. van der Minne, Electrostatics in the Petroleum Industry: The Prevention of Explosion Hazards. A Royal Dutch-Shell Research and Development Report, Elsevier Publishing Company, 1957.
[27] B.A. Yezer, A.S. Khair, P.J. Sides, D.C. Prieve, Determination of charge carrier concentration in doped nonpolar liquids by impedance spectroscopy in the presence of charge adsorption, J. Colloid Interf. Sci. 469 (2016) 325–337.
[28] K. Kon-no, A. Kitahara, Micelle formation of oil-soluble surfactants in nonaqueous solutions: effect of molecular structure of surfactants, J. Colloid Interf. Sci. 35 (4) (1971) 636–642.
[29] H.-F. Eicke, H. Christen, Is water critical to the formation of micelles in apolar media??, Helv Chim. Acta 61 (6) (1978) 2258–2263.
[30] E. Ruckenstein, R. Nagarajan, Aggregation of amphiphiles in nonaqueous media, J. Phys. Chem. 84 (11) (1980) 1349–1358.
[31] G.N. Smith, P. Brown, S.E. Rogers, J. Eastoe, Evidence for a critical micelle concentration of surfactants in hydrocarbon solvents, Langmuir 29 (10) (2013) 3252–3258.
[32] L.K. Shrestha, T. Sato, M. Dulle, O. Glatter, K. Aramaki, Effect of lipophilic tail architecture and solvent engineering on the structure of trehalose-based nonionic surfactant reverse micelles, J. Phys. Chem. B 114 (37) (2010) 12008–12017.
[33] M.E. Parent, J. Yang, Y. Jeon, M.F. Toney, Z.-L. Zhou, D. Henze, Influence of surfactant structure on reverse micelle size and charge for nonpolar electrophoretic inks, Langmuir 27 (19) (2011) 11845–11851.
[34] Y.-L. Lin, M.-Z. Wu, Y.-J. Sheng, H.-K. Tsao, Effects of molecular architectures and solvophobic additives on the aggregative properties of polymeric surfactants, J. Chem. Phys. 136 (10) (2012) 104905.
[35] H. Moon, S.K. Cho, R.L. Garrell, C.-J.C. Kim, Low voltage electrowetting-on-dielectric, J. Appl. Phys. 92 (7) (2002) 4080–4087.
[36] G.I. Taylor, Disintegration of water drops in an electric field, Proc. Roy. Soc. A-Math Phys. 280 (1382) (1964) 383–397.
[37] H. Nganguia, Y.-N. Young, P.M. Vlahovska, J. Blawzdziewicz, J. Zhang, H. Lin, Equilibrium electro-deformation of a surfactant-laden viscous drop, Phys. Fluids 25 (9) (2013) 092106.
[38] P.M. Vlahovska, Electrohydrodynamics of drops and vesicles, Annu. Rev. Fluid Mech. 51 (2019) 305–330.
[39] H. Nganguia, O.S. Pak, Y.-N. Young, Effects of surfactant transport on electrodeformation of a viscous drop, Phys. Rev. E 99 (6) (2019) 063104.
[40] M.D. Reichert, L.M. Walker, Coalescence behavior of oil droplets coated in irreversibly-adsorbed surfactant layers, J. Colloid Interf. Sci. 449 (2015) 480–487.
[41] S. Mhatre, S. Simon, J. Sjöblom, Methodology to calculate interfacial tension under electric field using pendent drop profile analysis, Proc. Roy. Soc. A-Math Phys. 475 (2225) (2019) 20180852.
[42] J.R. Turner, J. Thayer, Introduction to Analysis of Variance: Design, Analysis & Interpretation, Sage Publications, 2001.